


Dielectric and Magnetic Properties of Epoxy with Dispersed Iron Phosphate Glass Particles by Microwave Measurement

Sim Man Seng^{1,2} , Kok Yeow You² , Fahmiruddin Esa¹ , Mohd Zul Hilmi Mayzan^{1*} 

¹Ceramic and Amorphous Group (CerAm), Faculty of Applied Sciences and Technology, Pagoh Higher Education Hub, Universiti Tun Hussein Onn Malaysia, 84600 Panchor, Johor, Malaysia, simmanseng@gmail.com, fahmir@uthm.edu.my, zulhilmi@uthm.edu.my

²School of Electrical Engineering, Faculty of Engineering, Universiti Teknologi Malaysia, 81310 Johor Bahru, Johor, Malaysia, kyyou@fke.utm.my

Abstract— This paper investigates the dielectric properties and magnetic properties of epoxy composites with different amount of powdered iron phosphate glass (IPG) at 8.2 GHz to 12.4 GHz using microwave technique. IPG composed of 60P₂O₅-40Fe₂O₃ (mol%) was produced by conventional melt and quenching method and crushed into powder. The IPG powder was characterized using energy dispersive X-ray spectroscopy (EDS), particle size analyzer and powder X-ray diffraction (XRD). Different amount of IPG (10-70 wt%) were dispersed in the epoxy. The epoxy-IPG composites were characterized by their morphology, elemental composition and scattering parameters using scanning electron microscope (SEM), energy dispersive X-ray spectroscopy (EDS) and vector network analyzer (VNA), respectively. Reflection coefficient, $|S_{11}|$ increases whereas transmission coefficient, $|S_{21}|$ decreases with increasing IPG content in epoxy. Dielectric constant, ϵ_r' of epoxy-IPG composites were found increased with the IPG content from 3.33 to 4.69.

Index Terms— Dielectric properties, Magnetic properties, Iron phosphate glass, Epoxy, Composites.

I. INTRODUCTION

Phosphate glasses are chemical durable compared with most silicate and borosilicate glasses. The addition of iron to phosphate glasses strengthens the chemical bonds in the glass structure and further improves the chemical durability. This property allows iron phosphate glasses to be used in hazardous wastes immobilization [1]–[4]. Iron phosphate glasses exhibit low melting temperature (typically between 950 and 1150 °C). The batch materials of iron phosphate glasses couple well with microwave radiation. Therefore, microwave heating technique is introduced to produce iron phosphate glass [5], [6]. The technique is a fast and energy-saving alternative to the conventional heating technique using furnaces. The microwave radiation interacts with ions and dipoles in the batch materials, and increases their temperature to the melting point [7]. Besides using microwave to heat the batch materials, microwave can also be used to investigate various properties of glasses.

Several microwave measurement techniques such as free-space measurement [8], [9], coaxial probe measurement [10] and waveguide measurement [11], [12] have been employed to investigate

absorption characteristics, shielding effectiveness and dielectric properties of materials. The basic working principle of microwave measurement is based on the interaction between material and incident electromagnetic waves, including reflection, transmission and absorption. However, it is difficult to measure the properties of glasses using microwave measurement techniques because the material under test is normally required to be in specific dimensions and shapes. For instance, material in planar, toroid and rectangular shapes are normally required for free space, coaxial probe, and rectangular waveguide measurement techniques, respectively [13]. Despite this, glasses can be crushed into powders and introduced into polymeric matrices such as epoxy resin, paraffin wax and rubber. The mixture is in viscous liquid form and will solidify after curing in the mould of desired size and shape. Particle filled polymeric composites are often used due to easy preparation and low processing temperature [14]. The composites also provides flexibility in their geometrical design based on the geometry of the mould. In fact, the properties of particle filled polymeric composites were investigated for various applications [15]–[20].

Dielectric properties measurement of phosphate glasses are of considerable research interests because of their applications in various fields of materials science including semiconductors, photonic materials and biomedical materials [21]–[24]. In addition, the dielectric properties of phosphate glasses doped with iron oxides were investigated using microwave measurement technique [12]. Transmission line measurement technique was used to measure the microwave transmission and reflection of samples filled in rectangular waveguide in order to determine the relative complex permittivity and permeability [25]. Furthermore, iron phosphate glasses exhibit interesting electrical and magnetic properties depending on the iron coordination number in which the iron ions can exist in two oxidation states as Fe^{2+} and Fe^{3+} [26]. However, it is shown that the Fe^{2+} ions contribute effectively to the dielectric permittivity due to the interactions of the dipoles with the microwave radiation [27]. The polarization state of the composites can be evaluated by means of measurements of dielectric constant [28]. Although several works have been reported on the dielectric properties of conventional phosphate glasses doped with different transition elements, but there is not much information available on using microwave measurement technique to investigate the powdered iron phosphate glasses dispersed in a polymeric structure. Knowledge of the microwave effects on the glasses may suggest modifications on the composition and processing conditions, which possibly expand their applications.

In this paper, the dielectric properties and magnetic properties of the epoxy composites with dispersed powdered IPG of different composition ratios in X-band microwave frequency range are reported. Epoxy resin is used due to ease of preparation and flexibility in geometrical design. The measured properties of the epoxy-IPG composites can be used to predict the properties of pure IPG. The powdered IPG are characterized using energy dispersive X-ray spectroscopy (EDS), particle size analyzer and powder X-ray diffraction (XRD). The morphology, elemental composition and scattering parameters of the epoxy-IPG composites are investigated using scanning electron microscope (SEM),

energy dispersive X-ray spectroscopy (EDS) and vector network analyzer (VNA), respectively.

II. EXPERIMENTAL

A. Iron Phosphate Glass

The 60P₂O₅-40Fe₂O₃ (mol %) glass was prepared from sodium dihydrogen phosphate (NH₄H₂PO₄ – 98 % purity, Alfa Aesar) and magnetite (Fe₃O₄ – 97 % purity, Alfa Aesar) using conventional melt and quenching method. 200 g glass batch according to the nominal composition was weighed, mixed homogeneously and placed into a mullite crucible. The powders were heated at a heating rate of 2 °C/min in an electric box furnace (ELITE). The temperature was raised to 1150 °C for 3 hours and the molten glass was poured into a pre-heated stainless steel mould. The obtained glass block were then annealed for 1 hour at 450 °C and cooled to room temperature at a cooling rate of 1 °C/min.

Bulk density of the annealed glass was measured by Archimedes' principle at room temperature using density balance (XS64, Mettler Toledo). The glass was cut into monoliths of 5 x 5 x 20 mm using diamond cutter to be loaded into the dilatometer. Dilatometer (DIL 420C, Netzsch) with 3 °C/min heating rate was used to determine the glass transition temperature (T_g).

The annealed glass was then crushed using a stainless steel percussion mortar and sieved using a test sieve (<75 µm) to obtain powdered glass. Powder density was measured using a helium gas pycnometer (Micromeritics Accupyc II 1340). The chemical composition analysis was done using energy dispersive X-ray spectroscopy (EDS; JSM6400, JEOL). Particle size of the powdered IPG was examined using a laser diffraction particle size analyser (LS 130, Beckman Coulter).

X-ray diffractometer (XRD; D500, Siemens) analysis on the powders was performed to confirm the amorphous property of the glass. The detector operated at 40 kV and 30 mA, utilized the CuK_α radiation ($\lambda = 1.5406 \text{ \AA}$) and scanned over a 2θ range from 10° to 80° at 1°/min intervals with a step size of 0.05°.

B. Epoxy-Iron Phosphate Glass Composite

The epoxy-glass composite samples were prepared by curing the IPG powder in epoxy resin. Liquid epoxy resin (Der 331, Emory) were mixed with hardener (Jointmine 925-3, Emory) at a ratio of 2:1. The IPG powder were weighted according to its weight percentage in the composite (10-70 wt%) and added to the liquid mixture. The mixture was stirred with a glass rod and poured into an Aluminium sample holder with an opening of dimension 22.86 x 10.16 x 3.00 mm³ as shown in Fig. 1 (a). The mixture was cured for 24 h at room temperature. The samples were then grinded and polished for flat surface finishing.

Density balance (XS64, Mettler Toledo) was used to determine the bulk density of the epoxy composites. The morphologies and elemental analysis of selected samples were characterized using a scanning electron microscope (SEM; ProX, Phenom) attached with Energy dispersive spectroscope (EDS).

Vector Network Analyzer (VNA; E5071C, Keysight) was used to measure the complex reflection

coefficient, S_{11} and transmission coefficient, S_{21} of the epoxy-IPG composites. X-band rectangular waveguides as shown in Fig. 1 (b) were connected to the vector network analyzer via a pair of coaxial cables. Through-reflect-line (TRL) calibration were carried out before the measurement of the samples. Both S_{11} and S_{21} of the samples were measured from 8.2 GHz to 12.4 GHz.

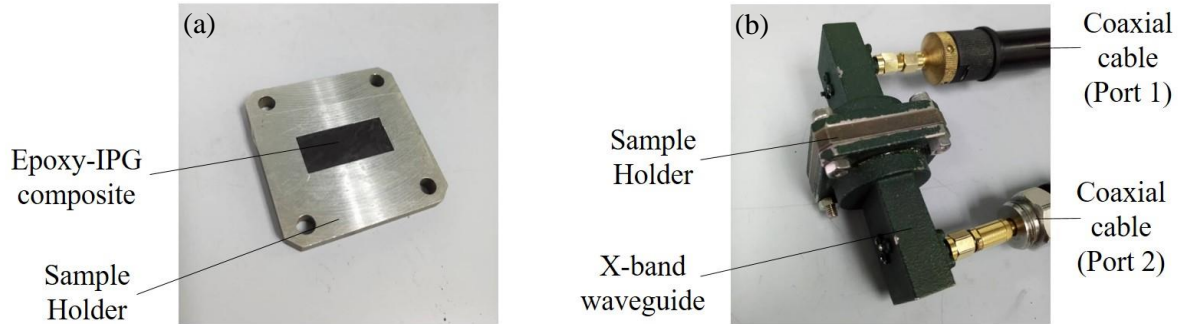


Fig. 1. (a) Sample holder containing epoxy-IPG composite, (b) X-band waveguide measurement setup

The measured S_{11} and S_{21} were used to retrieve the properties of the epoxy-IPG composites. Energy absorption coefficient, A of the composites was calculated using Equation (1).

$$A = 1 - |S_{11}|^2 - |S_{21}|^2 \quad (1)$$

Interfacial reflection coefficient, Γ and interfacial transmission coefficient, T were determined using Equation (2) and (3).

$$\Gamma = \frac{S_{11}^2 - S_{21}^2 + 1}{2S_{11}} \pm \sqrt{\left(\frac{S_{11}^2 - S_{21}^2 + 1}{2S_{11}}\right)^2 - 1} \quad (2)$$

$$T = \frac{S_{11} + S_{21} - \Gamma}{1 - (S_{11} + S_{21})\Gamma} \quad (3)$$

Hence, the relative complex permittivity, ϵ_r and permeability, μ_r of the composites were calculated using Nicolson-Ross-Weir (NRW) algorithm [29] as:

$$\epsilon_r = \frac{1}{\mu_r k_0^2} \left[4\pi^2 \left(\frac{1}{\Lambda}\right)^2 + k_c^2 \right] \quad (4)$$

$$\mu_r = \frac{2\pi}{\sqrt{k_0^2 - k_c^2}} \left(\frac{1}{\Lambda}\right) \left(\frac{1+\Gamma}{1-\Gamma}\right) \quad (5)$$

$$\frac{1}{\Lambda^2} = - \left[\frac{1}{2\pi d} \ln(T) \right]^2 \quad (6)$$

where k_0 is the free space wavenumber, k_c is the cut-off wavenumber and d is the thickness of the composite sample.

III. RESULTS AND DISCUSSION

A. Iron Phosphate Glass

The chemical compositions and physical properties of prepared IPG are listed in Table 1. The nominal composition of the prepared glass system was 60P₂O₅-40Fe₂O₃ (mol%), however 1.07 mol% of Al₂O₃ was detected by EDS. Contamination by Al was due to the corrosion of the mullite crucibles

by the glass melt at high temperature. Bulk density and powder density of the glass are $3.152 \pm 0.158 \text{ g/cm}^3$ and $3.1614 \pm 0.0009 \text{ g/cm}^3$ respectively. The glass transition temperature, T_g is $457 \pm 5 \text{ }^\circ\text{C}$. The average particle diameter of the glass powder is $34.8 \pm 1.7 \text{ }\mu\text{m}$ measured by volume basis and $0.76 \pm 0.04 \text{ }\mu\text{m}$ measured by number basis.

TABLE I. CHEMICAL COMPOSITIONS AND PHYSICAL PROPERTIES OF IRON PHOSPHATE GLASS

Oxide	Nominal composition (mol%)	Measured composition by EDS (mol%)
Al ₂ O ₃	-	1.07
Fe ₂ O ₃	60	59.93
P ₂ O ₅	40	39.00
Total	100	100.00
Bulk density (g/cm ³)		3.152 ± 0.158
Powder density (g/cm ³)		3.1614 ± 0.0009
T_g (°C)		
DIL 420C		457 ± 5
Average particle size (Diameter/ μm)		
Volume basis		34.8 ± 1.7
Number basis		0.76 ± 0.04

The XRD pattern in Fig. 2 shows diffuse scattering behavior without any crystalline peaks and this confirmed the amorphous character of the glass, which has a random arrangement of atoms.

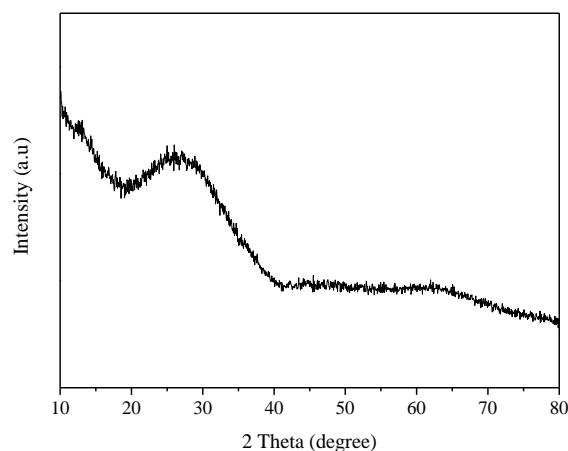


Fig. 2. X-ray diffraction pattern of powdered iron phosphate glass

B. Epoxy-Iron Phosphate Glass Composites

Based on Fig. 3, the bulk density of the epoxy-glass composites increases when the glass content in the composite increases from 0 to 70 wt%. The density of the sample without glass filler is $1.1725 \pm 0.0007 \text{ g/cm}^3$ whereas the density of the sample containing 70 wt% of glass content is $1.8966 \pm 0.0032 \text{ g/cm}^3$. The bulk density of the epoxy-IPG composite increases when IPG content increases because the density of IPG is higher than that of epoxy.

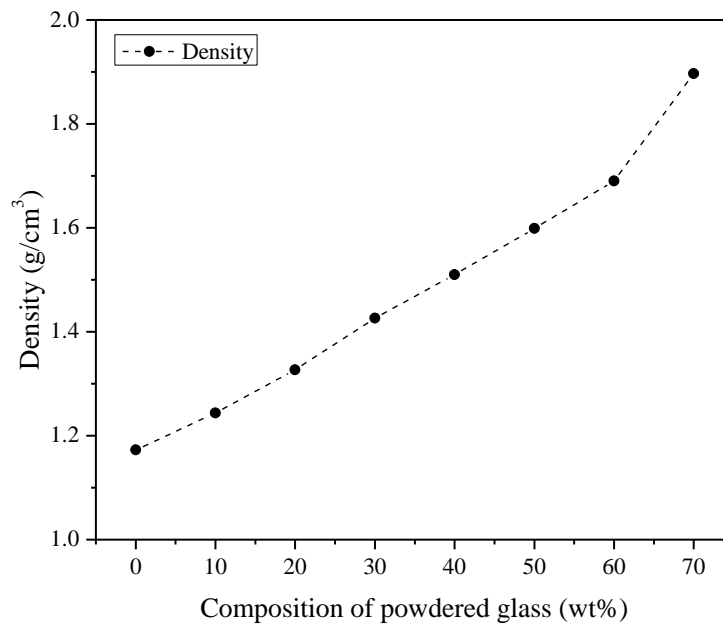


Fig. 3. Density of epoxy-IPG composites of different composition

Fig. 4 shows the SEM micrographs of three selected epoxy-IPG composites samples having 10 wt%, 30 wt% and 70 wt% of IPG. There are bright and dark regions being observed in all the micrographs. The bright regions were confirmed by EDS [refer Fig. 5 (d)] to be IPG particles and the dark region is epoxy matrix. The distribution of the IPG particles in epoxy matrix is illustrated in the micrographs. The glass particles were more concentrated with the increasing of glass content, which was also indirectly proven using the density result (refer Fig. 3).

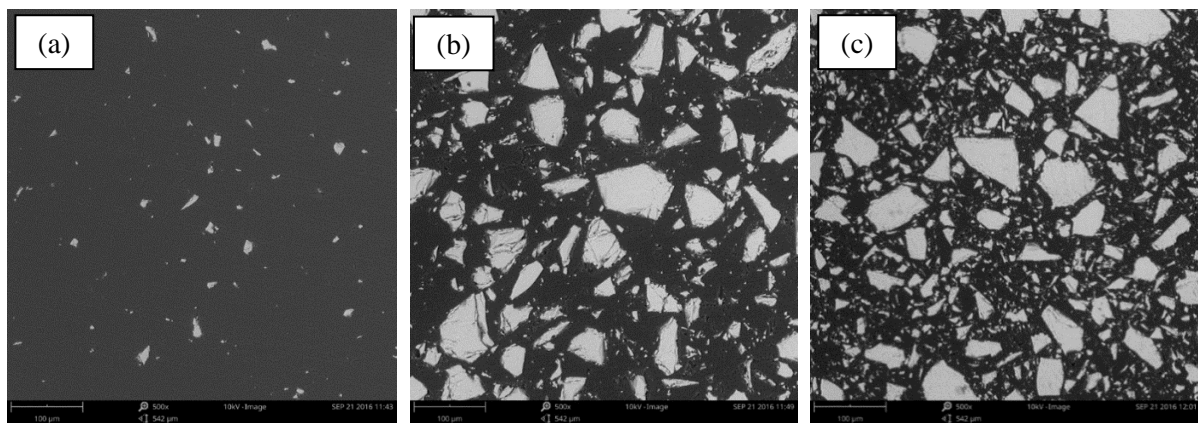


Fig. 4. SEM micrographs of epoxy-IPG composites containing (a) 10 wt%, (b) 30 wt%, (c) 70 wt% of powdered IPG.

Fig. 5 (a)-(c) shows the position of spots (denoted by A, B, C, D, E, and F) which were examined by EDS on the selected epoxy-IPG composites. Fig. 5 (d) shows the EDS spectra of the spots. Spots A, C and E (bright regions) are identified as IPG as they contain P, Fe, and O. However, a slight amount of C and N were also detected in these regions because the penetration volume in the detection spots might include the epoxy matrix due to the small particle size of glass. For the dark region, spot B is found to have C, N and O only but there were also detection of P and Fe for spots D

and F. Higher concentration of glass particles was responsible for the detection of P and Fe as the penetration volume might reach the glass particles beneath the epoxy surface that were invisible from the surface.

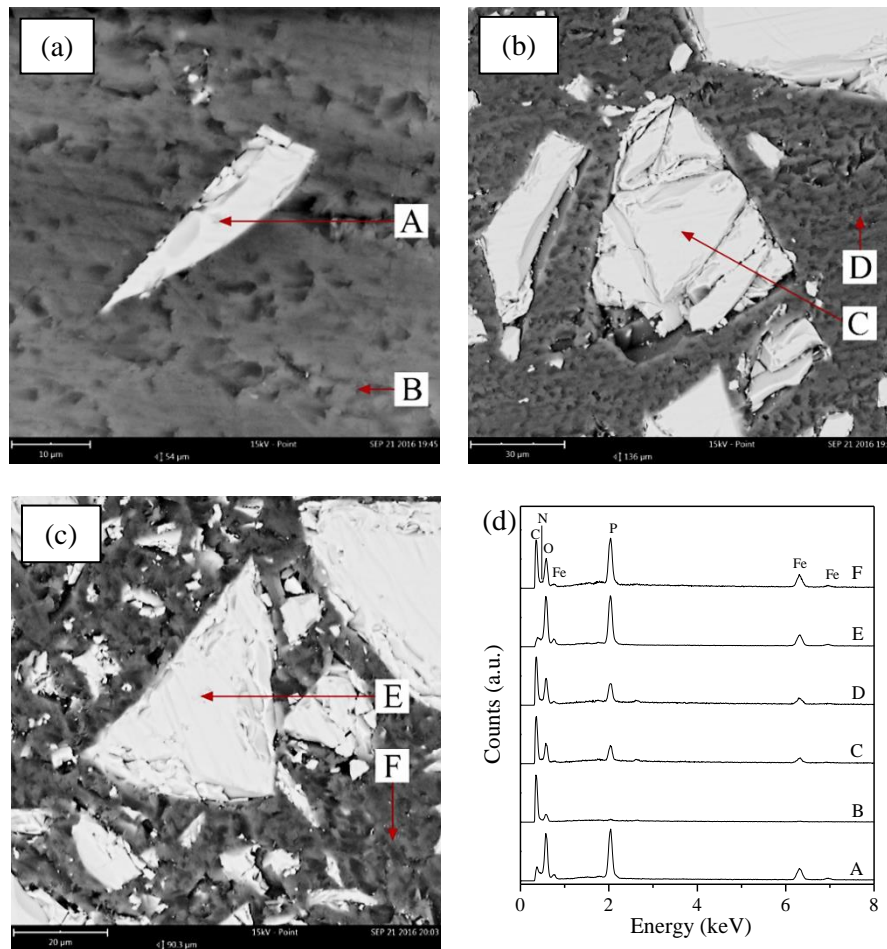


Fig. 5. EDS spot analysis on epoxy-IPG composites containing (a) 10 wt%, (b) 30 wt%, (c) 70 wt% of powdered IPG; and their (d) EDS spectra

Fig. 6 (a) and (b) show the linear magnitude of reflection coefficient, $|S_{11}|$ and transmission coefficient, $|S_{21}|$ of the epoxy-IPG composite samples in the X-band frequency range, respectively. Based on Fig. 6 (a), the measured $|S_{11}|$ increases when the content of powdered IPG inside the epoxy resin increases. $|S_{11}|$ increases due to the mismatch between the impedance of the composites and the characteristic impedance of waveguide [30]. The impedance mismatch causes the reflection of the electromagnetic signals. Based on Fig. 6 (b), the measured $|S_{21}|$ has an opposite trend compared with $|S_{11}|$, in which its magnitude decreases when the IPG content increases. There are less transmitted signals (more reflected signals) for composites with higher IPG content. In other words, IPG is a better electromagnetic energy reflector than the epoxy.

Since the measurement used in this work is a closed system technique, absorption coefficient, $|A|$ can be determined using Equation (1). $|A|$ is a parameter to determine the magnitude of incident microwave energy being absorbed and dissipated by the material. Fig. 6 (c) shows the linear magnitude of absorption coefficient, $|A|$. In general, $|A|$ of the epoxy-IPG composites are all below

0.08. This shows that the absorption capabilities of the composites are insignificant (below ~8 % of the incident energy is absorbed). The incident electromagnetic waves undergo partial reflection and partial transmission with negligible absorption. The composites do not resonate with the electromagnetic wave at X-band frequency range. However, epoxy without IPG fillers exhibits the highest $|A|$ compared with other epoxy-IPG composites. The absorption mechanism of the epoxy is based on its dielectric loss mechanism. Dipole polarization occurs and always lags behind the electrical field inducing it [31]. This lags results in the energy dissipation.

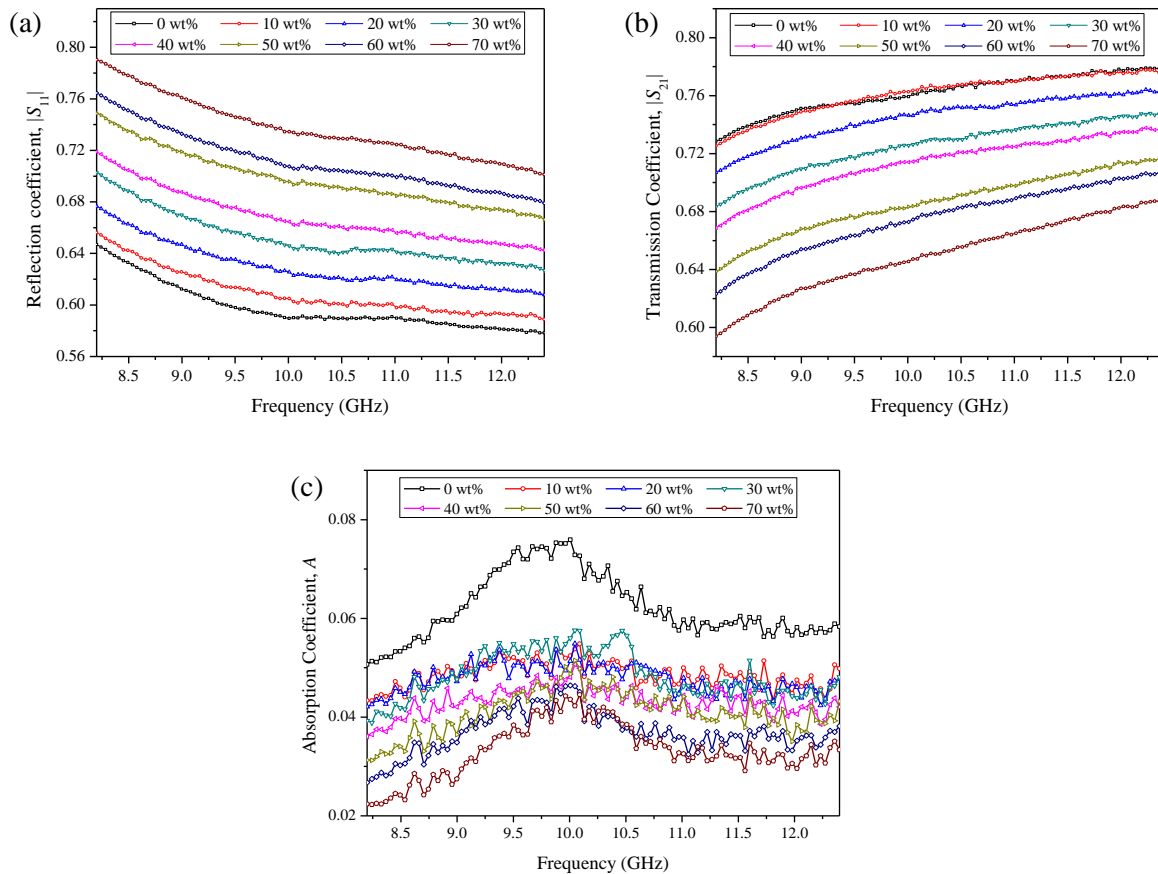


Fig. 6. Frequency dependences of linear magnitude of (a) reflection coefficient $|S_{11}|$, (b) transmission coefficient, $|S_{21}|$, (c) absorption coefficient, $|A|$

Relative complex permittivity, ϵ_r and relative complex permeability, μ_r of composite samples were calculated using Nicolson-Ross-Weir (NRW) conversion technique based on the measured S_{11} and S_{21} [29], [32], [33]. The series of curves in Fig. 7 (a) show that the real part of relative permittivity, ϵ_r' (so-called dielectric constant) increases when the IPG content in the composite increases. The average values of ϵ_r' were 3.27, 3.33, 3.50, 3.72, 3.86, 4.18, 4.35 and 4.69 for corresponding epoxy composites containing 0 wt% (without IPG content), 10 wt%, 20 wt%, 30 wt%, 40 wt%, 50 wt%, 60 wt% and 70 wt% of IPG, respectively. The dielectric behaviour is associated with the polarization phenomena. The interfacial polarization phenomena which usually occurs in amorphous solid determines the dielectric behaviour [34]. The addition of IPG increases the number of interfaces in the composites

[35]. The interfacial polarization, which is caused by the accumulation of charges at the interfaces between IPG and epoxy, is enhanced [36]. The presence of intrinsic dipoles formed by charged pairs contributes to the increment of dielectric constant [28], [37].

The imaginary part of relative complex permittivity, ϵ_r'' (so-called dielectric loss factor) is in the range of 0.04 to 0.18 as shown in Fig 7 (b). In general, ϵ_r' is a measure of how much energy from an external electromagnetic field can be stored in a material whereas ϵ_r'' represents how dissipative a material is to the external electromagnetic field. ϵ_r'' of the IPG-composites is low ($\epsilon_r'' < 0.18$) and this leads to negligible dissipation of energy in the composites [refer Fig. 6 (c)]. This low dielectric loss property allows IPG to be used in X-band frequency applications because the dissipation of energy into heat is negligible. Energy loss or energy absorption is avoided while taking advantages of the desirable mechanical properties of IPG including high corrosive resistance, high melting point, hard and durable. For instance, IPG can be potentially used as insulating support structures in microwave applications.

Relative complex permeability, μ_r is a measure of the material related to its magnetic interactions with the incoming electromagnetic wave. Since both IPG and epoxy resin are non-magnetic materials, the real part of relative permeability, μ_r' of the composites show unity value ($\mu_r' \approx 1$) at X-band frequency range. Based on Fig. 7 (c), μ_r' fluctuated in the range of 0.99 to 1.04. The imaginary part of relative permeability, μ_r'' is approximately zero ($\mu_r'' \approx 0$) for all the composite samples as shown in Fig. 7 (d). Electric loss tangent, $\tan \delta_e$ and magnetic loss tangent, $\tan \delta_m$ are shown in Fig. 7 (e) and (f). The results show that there are very less of loss caused by dielectric and magnetic loss mechanisms inside the composite samples. This result is supported by the absorption curve in Fig. 6 (c) which shows that the composite samples exhibit low energy absorption. The absorption coefficient results show that the microwave radiation in the X-band frequency range could not be absorbed by any glassy phase even though there are Fe_2O_3 in the IPG. Hence, IPG can be considered as a non-microwave interactive material at X-band frequency range although its batch materials are a good microwave absorber at certain frequency. This property makes IPG a safer candidate in hazardous wastes immobilization.

Based on Fig. 7 (a), ϵ_r' has considerable consistency of increment trend with each 10 wt% increment of IPG filler content. This proves the applicability of the measurement technique in developing a permittivity sensor for micro-sized particles. ϵ_r' of the particles can be predicted by measuring S_{11} and S_{21} of the particles in polymers. Particle-filled polymeric composites can be used to predict the properties of particle fillers which are difficult to be handled in powder form in microwave measurement.

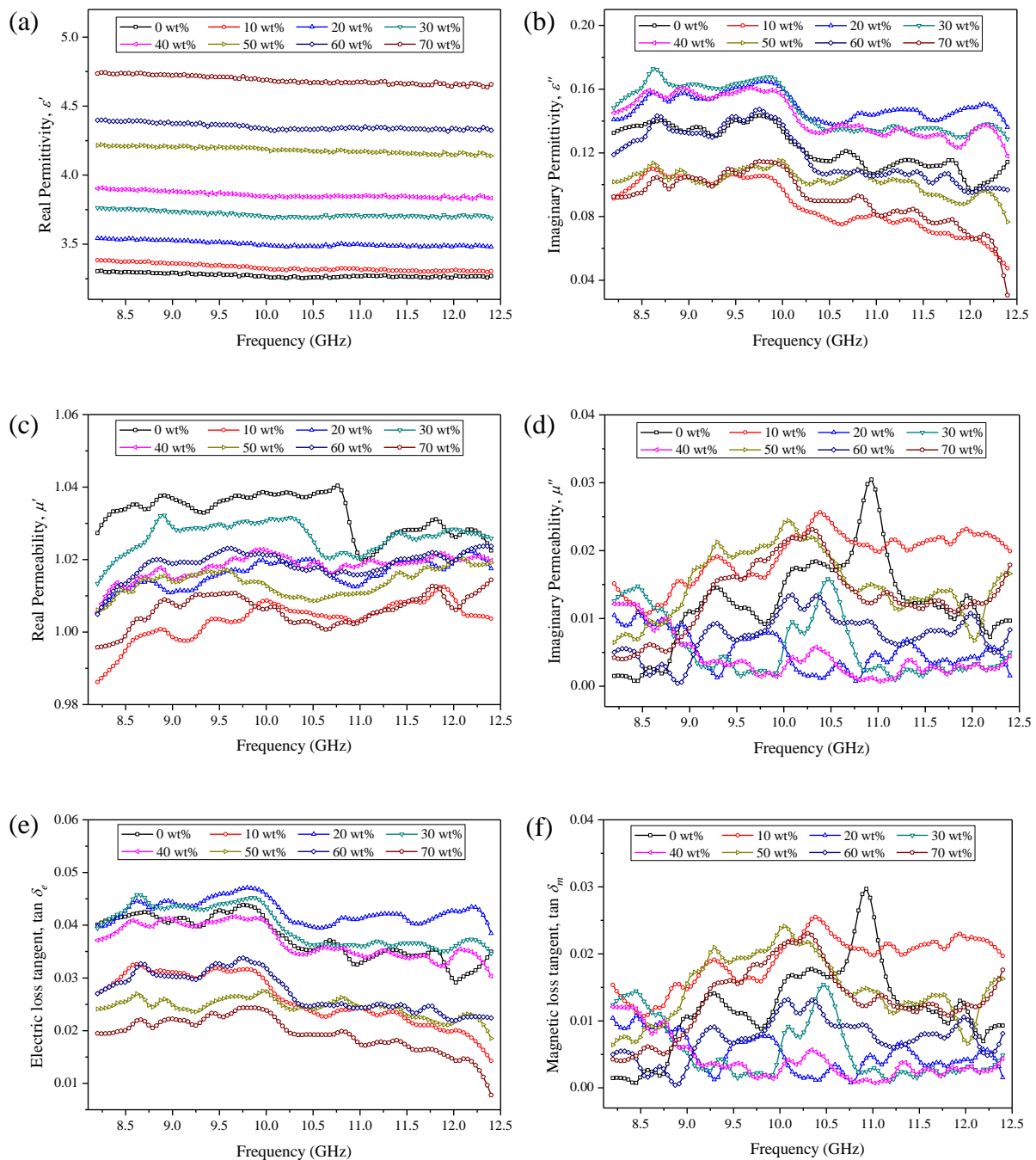


Fig. 7. Frequency dependences of (a) real permittivity, (b) imaginary permittivity, (c) real permeability, (d) imaginary permeability, (e) electric loss tangent, (f) magnetic loss tangent

IV. CONCLUSION

Epoxy-iron phosphate glass composites of different composition ratios were prepared. The determination of the electromagnetic properties of the composites were demonstrated using rectangular waveguide in the X-band frequency range. Several characterization techniques were conducted to investigate the density, morphology, elemental composition and scattering parameters. Relative complex permittivity, ϵ_r' are 3.27, 3.50, 3.86, and 4.35 for epoxy-IPG composites having 0, 20, 40, and 60 wt% of IPG, respectively. Relative complex permeability, μ_r' are all near unity. The

microwave absorption is near-zero and there is negligible loss of microwave energy in the composite materials.

REFERENCES

- [1] K. Xu, P. Hrma, W. Um, and J. Heo, "Iron phosphate glass for immobilization of ^{99}Tc ," *J. Nucl. Mater.*, vol. 441, no. 1–3, pp. 262–266, 2013.
- [2] M. Z. H. Mayzan, M. C. Stennett, N. C. Hyatt, and R. J. Hand, "Graphite immobilisation in iron phosphate glass composite materials produced by microwave and conventional sintering routes," *J. Nucl. Mater.*, vol. 454, no. 1–3, pp. 343–351, 2014.
- [3] P. Stoch, M. Ciecinska, and A. Stoch, "Thermal properties of phosphate glasses for salt waste immobilization," *J. Therm. Anal. Calorim.*, vol. 117, no. 1, pp. 197–204, 2014.
- [4] X. Liu, Y. Qiao, Z. Qian, and H. Ma, "Research on chemical durability of iron phosphate glass wastefoms vitrifying SrF_2 and CeF_3 ," *J. Nucl. Mater.*, vol. 508, pp. 286–291, 2018.
- [5] N. H. M. Farhadi, R. Rosli, M. I. Kimpa, F. Esa, M. H. Ismail, and M. Z. H. Mayzan, "Synthesis and Properties of Zinc Iron Phosphate Glasses Prepared by Microwave and Conventional Processing Methods," *J. Sci. Technol.*, vol. 9, no. 3, pp. 87–91, 2017.
- [6] A. K. Mandal, S. Sen, S. Mandal, C. Guha, and R. Sen, "Energy Efficient Melting of Glass for Nuclear Waste Immobilization Using Microwave Radiation," *Int. J. Green Energy*, vol. 12, no. 12, pp. 1280–1287, 2015.
- [7] F. J. M. Almeida, J. R. Martinelli, and C. S. M. Partiti, "Characterization of iron phosphate glasses prepared by microwave heating," *J. Non. Cryst. Solids*, vol. 4783–4791, 2007.
- [8] S. S. Afghahi, M. Jafarian, and C. A. Stergiou, "X-band microwave absorbing characteristics of multicomponent composites with magnetodielectric fillers," *J. Magn. Magn. Mater.*, vol. 419, pp. 386–393, 2016.
- [9] J. H. Oh, K. S. Oh, C. G. Kim, and C. S. Hong, "Design of radar absorbing structures using glass/epoxy composite containing carbon black in X-band frequency ranges," *Compos. Part B Eng.*, vol. 35, no. 1, pp. 49–56, 2004.
- [10] K. Y. You, Z. Abbas, C. Y. Lee, M. F. A. Malek, K. Y. Lee, and E. M. Cheng, "Modeling and measuring dielectric constants for very thin materials using a coaxial probe," *Radioengineering*, vol. 23, no. 4, pp. 1016–1025, 2014.
- [11] K. Y. You, Z. Abbas, M. F. A. Malek, and E. M. Cheng, "Non-destructive dielectric measurements and calibration for thin materials using waveguide-coaxial adaptors," *Meas. Sci. Rev.*, vol. 14, no. 1, pp. 16–24, 2014.
- [12] P. Bergo, W. M. Pontuschka, J. M. Prison, and C. C. Motta, "Investigation of some dielectric properties of phosphate glasses doped with iron oxides, by a microwave technique," *Measurement*, vol. 43, no. 2, pp. 210–215, 2010.
- [13] K. Y. You, "Materials Characterization Using Microwave Waveguide System," in *Microwave Systems and Applications*, 2017, pp. 341–358.
- [14] Y. Qing, W. Zhou, F. Luo, and D. Zhu, "Microwave-absorbing and mechanical properties of carbonyl-iron/epoxy-silicone resin coatings," *J. Magn. Magn. Mater.*, vol. 321, pp. 25–28, 2009.
- [15] T. K. Bindu Sharmila, J. V. Antony, M. P. Jayakrishnan, P. M. Sabura Beegum, and E. T. Thachil, "Mechanical, thermal and dielectric properties of hybrid composites of epoxy and reduced graphene oxide/iron oxide," *Mater. Des.*, vol. 90, pp. 66–75, 2016.
- [16] K. Devendra and T. Rangaswamy, "Strength Characterization of E-glass Fiber Reinforced Epoxy Composites with Filler Materials," *J. Miner. Mater. Charact. Eng.*, vol. 01, no. 06, pp. 353–357, 2013.
- [17] I. Kranauskaite, J. Macutkevicius, P. Kuzhir, N. Volynets, A. Paddubskaya, D. Bychanok, S. Maksimenko, J. Banys, R. Juskenas, S. Bistarelli, A. Cataldo, F. Micciulla, S. Bellucci, V. Fierro, and A. Celzard, "Dielectric properties of graphite-based epoxy composites," *Phys. Status Solidi Appl. Mater. Sci.*, vol. 211, no. 7, pp. 1623–1633, 2014.
- [18] A. Plyushch, J. Macutkevicius, P. Kuzhir, J. Banys, D. Bychanok, P. Lambin, S. Bistarelli, A. Cataldo, F. Micciulla, and S. Bellucci, "Electromagnetic properties of graphene nanoplatelets/epoxy composites," *Compos. Sci. Technol.*, vol. 128, pp. 75–83, 2016.
- [19] B. P. Singh, Prasanta, V. Choudhary, P. Saini, S. Pande, V. N. Singh, and R. B. Mathur, "Enhanced microwave shielding and mechanical properties of high loading MWCNT-epoxy composites," *J. Nanoparticle Res.*, vol. 15, no. 4, 2013.
- [20] Y. L. Chan, F. Esa, K. Y. You, M. S. Sim, M. Z. H. Mayzan, and M. A. Jusoh, "Electromagnetic properties of magnetite/epoxy resin composites at X-band frequency," in *Progress in Electromagnetics Research Symposium*, 2017, vol. 2017–Novem, pp. 3004–3010.
- [21] M. A. Valente, L. Bih, and M. P. F. Graça, "Dielectric analysis of tungsten–phosphoniobate $20\text{A}_2\text{O}-30\text{WO}_3-10\text{Nb}_2\text{O}_5-40\text{P}_2\text{O}_5$ (A=Li, Na) glass–ceramics," *J. Non. Cryst. Solids*, vol. 357, no. 1, pp. 55–61, 2011.
- [22] R. M. M. Morsi and S. Ibrahim, "Effect of Li_2O on the structure, electrical and dielectric properties of $x\text{Li}_2\text{O} \cdot (20-x)\text{CaO} \cdot 30\text{P}_2\text{O}_5 \cdot 30\text{V}_2\text{O}_5 \cdot 20\text{Fe}_2\text{O}_3$ glasses," *Phys. B*, vol. 406, pp. 2982–2989, 2011.
- [23] M. Shapaan, E. R. Shabaan, and A. G. Mostafa, "Study of the hyperfine structure, thermal stability and electric–dielectric properties of vanadium iron phosphate glasses," *Phys. B*, vol. 404, pp. 2058–2064, 2009.
- [24] P. Bergo, W. M. Pontuschka, J. M. Prison, and C. C. Motta, "Microwave insertion loss measurements in phosphate glasses containing transition metal oxides," *Meas. Sci. Technol.*, vol. 17, no. 4, pp. 855–858, 2006.
- [25] J. Baker-jarvis, R. G. Geyer, and P. D. Domich, "A Nonlinear Least-Squares Solution with Causality Constraints Applied to Transmission Line Permittivity and Permeability Determination," *IEEE Trans. Instrum. Meas.*, vol. 41, no. 5, pp. 646–652, 1992.
- [26] L. Zhang, R. K. Brow, M. E. Schlesinger, L. Ghussn, and E. D. Zanotto, "Glass formation from iron-rich phosphate melts," *J. Non. Cryst. Solids*, vol. 356, no. 25–27, pp. 1252–1257, 2010.

- [27] P. Bergo, W. M. Pontuschka, and J. M. Prison, "Dielectric properties and physical features of phosphate glasses containing iron oxide," *Mater. Chem. Phys.*, vol. 108, pp. 142–146, 2008.
- [28] P. Bergo, W. M. Pontuschka, J. M. Prison, C. C. Motta, and J. R. Martinelli, "Dielectric properties of barium phosphate glasses doped with transition metal oxides," *J. Non. Cryst. Solids*, vol. 348, pp. 84–89, 2004.
- [29] A. M. Nicolson, "Measurement of the Intrinsic Properties of Materials by Time-Domain Techniques," *IEEE Trans. Instrum. Meas.*, vol. 19, no. 8, pp. 377–382, 1970.
- [30] E. M. Cheng, M. S. A. Majid, S. A. Bakar, N. F. M. Nasir, S. F. Khor, K. Y. You, K. Y. Lee, M. R. M. Jamir, W. H. Tan, S. R. Shaharuddin, and C. Y. Beh, "Hardened Glass Particle and Carbon Black Using Resin for Potential Electromagnetic Shielding in Biomedical Electronic Equipments," *J. Phys. Conf. Ser.*, vol. 1372, no. 1, pp. 1–8, 2019.
- [31] A. K. Tagantsev and S. Federal, *Mechanisms of Dielectric Loss in Insulating Materials*, vol. 1. Elsevier Ltd., 2016.
- [32] A. L. De Paula, M. C. Rezende, and J. J. Barroso, "Modified Nicolson-Ross-Weir (NRW) method to retrieve the constitutive parameters of low-loss materials," in *Microwave & Optoelectronics Conference (IMOC)*, 2011, pp. 488–492.
- [33] O. Luukkonen, S. I. Maslovski, and S. a. Tretyakov, "A Stepwise Nicolson-Ross-Weir-Based Material Parameter Extraction Method," *IEEE Antennas Wirel. Propag. Lett.*, vol. 10, no. 3, pp. 1295–1298, 2011.
- [34] H. Sun, H. Zhang, S. Liu, N. Ning, and L. Zhang, "Interfacial polarization and dielectric properties of aligned carbon nanotubes/ polymer composites: The role of molecular polarity," *Compos. Sci. Technol.*, vol. 154, pp. 145–153, 2018.
- [35] K. Chen, X. Li, D. Lv, F. Yu, Z. Yin, and T. Wu, "Study on microwave absorption properties of metal-containing foam glass," *Mater. Sci. Eng. B*, vol. 176, no. 15, pp. 1239–1242, 2011.
- [36] X. Li, D. Lv, and K. Chen, "Effects of graphite additive on dielectric properties and microwave absorption properties of zinc-containing foam glass," *J. Non. Cryst. Solids*, vol. 358, no. 21, pp. 2917–2921, 2012.
- [37] A. Mogus-Milankovic and D. E. Day, "Thermally stimulated polarization and dc conduction in iron phosphate glasses," *J. Non. Cryst. Solids*, vol. 162, pp. 275–286, 1993.